Published in final edited form as:
Neuroimage. 2011 January 15; 54(2): 1188–1195. doi:10.1016/j.neuroimage.2010.08.043.

Regional Reproducibility of Pulsed Arterial Spin Labeling Perfusion Imaging at 3T

Wang Yang[1], **Andrew J. Saykin**[1], **Josef Pfeuffer**[2], **Chen Lin**[1], **Kristine M. Mosier**[1], **Li Shen**[1], **Sungeun Kim**[1], and **Gary D. Hutchins**[1]

[1]IU Center for Neuroimaging and Indiana Institute for Biomedical Imaging Sciences, Department of Radiology and Imaging Sciences, Indiana University School of Medicine, Indianapolis, IN, USA

[2]Siemens Healthcare, MR Applications Development, Erlangen, Germany

Abstract

Arterial spin labeling (ASL) is a promising non-invasive magnetic resonance imaging (MRI) technique for measuring regional cerebral blood flow (rCBF) or perfusion *in vivo*. To evaluate the feasibility of ASL as a biomarker for clinical trials, it is important to examine test-retest reproducibility. We investigated both inter- and intra-session reproducibility of perfusion MRI using a pulsed ASL (PASL) sequence PICORE Q2TIPS with an echo-planar imaging (EPI) readout. Structural MRI regions of interest (ROIs) were extracted individually by automated parcellation and segmentation methods using FreeSurfer. These cortical and subcortical ROIs were used to assess regional perfusion stability. Our results indicated regional variability in grey matter rCBF. Although rCBF measurements were characterized by intersubject variation, our results also indicated relatively less within-subject variability estimated as within-subject standard deviation (SD_W) (intersession SD_W: 2.0 to 8.8; intrasession SD_W: 2.8 to 9.6) and acceptable reliabilities as measured using intraclass correlation coefficient (ICC) (intersession ICC: 0.68 to 0.94; intrasession ICC: 0.66 to 0.95) for regional MRI perfusion measurements using the PICORE Q2TIPS technique. Overall, our findings suggest that PASL is a technique with good within and between session reproducibility. Further reproducibility studies in target populations relevant for specific clinical trials of neurovascular related agents will be important and the present results provide a framework for such assessments.

Keywords

Arterial spin labelling; Cerebral blood flow; Reproducibility; Magnetic resonance imaging

1. Introduction

The term cerebral perfusion refers to the process involved in delivery of nutrients and oxygen from arterial blood to the capillary system within the brain parenchyma, which is a fundamental and essential physiological entity of critical importance for the survival of brain tissue because it supports the brain's energy metabolism for subserving normal function. Cerebral blood flow (CBF) is a measure of the rate of delivery of arterial blood to a capillary

Corresponding Author: Yang Wang, M.D., Department of Radiology and Imaging Sciences, Indiana University School of Medicine, 950 W. Walnut St., R2 E124, Indianapolis, IN 46202, Phone: 317-278-3013, Fax: 317-274-1067, ywang1@iupui.edu.

bed in tissue. CBF parameters, in addition to being of interest, markers of vascular function, can be combined with other physiological measurements to reveal the complex neurobiology of healthy and disordered brain function. CBF measurements have been used as biomarkers of neural activity in cognitive and clinical neuroscience studies (Detre et al., 2009; Liu and Brown, 2007; Petersen et al., 2006). Numerous imaging techniques using either exogenous or endogenous tracers have been developed and applied to measure regional CBF (rCBF) (Wintermark et al., 2005). However, nuclear medicine based techniques such as positron emission tomography (PET) or single photon emission computed tomography (SPECT) using radioactive tracers have several disadvantages: high cost, invasive, ionizing radiation and limited repetition of acquisitions (Hermes et al., 2007; Wintermark et al., 2005). Therefore, MRI based perfusion imaging techniques potentially can provide an attractive alternative, because of their noninvasive nature, repeatability, availability of complementary anatomic and functional MRI scans, and superior temporal and spatial resolution compared to PET and SPECT. Two main MRI perfusion methods are currently available: dynamic susceptibility contrast (DSC) MRI which employs bolus tracking after the injection of an exogenous endovascular tracer and arterial spin labeling (ASL). Unlike the DSC MRI method, ASL requires no exogenous contrast and uses magnetically labeled arterial blood water as an endogenous tracer (Detre et al., 1992). The complete non-invasiveness of ASL makes it very suitable for perfusion studies of healthy participants and in patient groups requiring longitudinal investigations. This is especially important in patients with particular conditions, such as kidney failure, or in pediatric populations where the use of radioactive tracers or exogenous contrast agents may be restricted (Petersen et al., 2006).

In ASL, a perfusion-weighted image is generated by subtracting an image with magnetic labeling (label image) from an image without this labeling (control image). Several methods exist for ASL (Detre et al., 2009). In pulsed ASL (PASL), blood within an inversion volume is instantaneously inverted (Wong et al., 1998), whereas in continuous ASL (CASL), blood flowing through a specified plane is inverted continuously, most typically by flow driven adiabatic fast passage (Williams et al., 1992) or by pseudo-continuous labeling (pCASL) (Dai et al., 2008; Wu et al., 2007a). Similar to PET, ASL allows the quantification of rCBF in physiological units (ml of blood/100 g of tissue/min), both at rest as well as during activation. Validation studies have shown that ASL measurement has excellent concurrent validity when correlated with rCBF measured by PET (Donahue et al., 2006; Xu et al., 2010) or DSC MRI (Liu and Brown, 2007). The measurement of rCBF using ASL perfusion MRI provides a noninvasive means of quantifying regional brain function both at rest and in response to pharmacological or task-induced activation (Brown et al., 2007; Detre et al., 2009). ASL perfusion MRI measurements have been reported to be stable over time and have a lower inter-subject variation than blood oxygenation level dependent (BOLD) functional MRI (Tjandra et al., 2005; Wang et al., 2003a). ASL therefore appears potentially well-suited to longitudinal studies of normal development, degenerative diseases, or therapeutic interventions (Detre et al., 2009).

Despite the considerable progress over the past decade, application of ASL techniques has not overtaken traditional invasive rCBF measurement methods. One reason for this is the intrinsically low signal-to-noise ratio (SNR) in ASL measurements which attenuate sensitivity of the technique (Petersen et al., 2006). The low SNR mainly results from the small difference signal in the perfusion images, which could be as little as 1% of the static tissue signal (Wong et al., 1999). This is particularly crucial in functional activation studies. In resting state ASL measurements, the SNR can be increased by averaging over consecutive images (Liu and Brown, 2007; Petersen et al., 2006). Nevertheless, determination of reproducibility of ASL measurements as a function of time in healthy volunteer and its suitability to consistently detect differences between regions in resting state

is critical prior to use in pharmacological and longitudinal studies of patient populations (Hermes et al., 2007).

Recently, several groups have conducted such reproducibility studies of resting state ASL measurements using different ASL schemes, such as PASL (Cavusoglu et al., 2009; Jahng et al., 2005; Petersen et al., 2010; Yen et al., 2002), CASL (Floyd et al., 2003; Gevers et al., 2009; Hermes et al., 2007; Parkes et al., 2004) or pCASL (Xu et al., 2010). While all these studies mainly focused on reproducibility of rCBF measurement of cortical grey matter (GM) as a whole, very few reported additional analysis on lobar region-of-interest (ROI) derived from published template (Hermes et al., 2007; Xu et al., 2010). Some reports examined manually outlined flow territories of the right and left anterior, middle, and posterior cerebral arteries on the basis of other published templates (Floyd et al., 2003; Gevers et al., 2009; Hermes et al., 2007; Yen et al., 2002). Although all these studies found that the reproducibility was comparable to other rCBF imaging techniques such as PET or SPECT, it is unknown if specific anatomical/functional regions will show as good, better or diminished reliability relative to the typically reported whole GM rCBF. Although theoretically a larger ROI might be expected to show greater reliability, there is some evidence to suggest that analysis of ASL data based on a large ROIs may suffer from inaccuracies arising from a distribution of transit times (Figueiredo et al., 2005).

A close coupling between rCBF and metabolism allows regional brain function to be assessed through measurements of cerebral perfusion and is the basis for a broad range of potential applications as a biomarker of regional brain function in basic and clinical neuroscience (Detre et al., 2009). For instance, ASL perfusion MRI is sensitive to changes in local rCBF and metabolism that occur in degenerative diseases, including Alzheimer's dementia (Alsop et al., 2008) and frontotemporal dementia (Du et al., 2006). Thus, it is becoming increasingly important to characterize reliability of ASL measurement in different subdivisions of neocortical and subcortical areas. Recently, Asllani et al. found substantial intrasubject systematic variability in rCBF of GM ROIs in their study, which were primarily restricted to selected ROIs based on a commonly used template (Asllani et al., 2008b). Another important element of reproducibility is the comparison of stability with a single scan session compared to test-retest stability over an intervening interval. To date no studies have examined the regional reproducibility of PASL measurements both within- and between scan sessions. The aim of the present study was to extend prior test-retest reproducibility studies of resting state PASL measurements to address two issues: (1) within-session vs. one week retest reproducibility and (2) regional variation in reproducibility of PASL using standardized and automated ROIs extracted from morphometric MRI.

2. Materials and Methods

2.1. Procedure

This study was approved by the local Institutional Review Board, and all subjects provided written informed consent before participating. Ten healthy subjects (mean±SD age = 27 ± 8 years, male/female = 5/5) were scanned in two sessions with an interval of one week. To minimize effects of diurnal variations in baseline rCBF, each session for a particular subject was acquired at the same time of same day in two sequential weeks. Subjects were asked to make sure that intake of caffeine, as well as amount of sleep was equal before each MRI exam. The MR scans of all subjects in this project were completed over a 6-week period. Scanner stability is assessed on a daily basis in our center including this 6-week period.

2.2. Data acquisition

MR measurements were acquired on a 3T whole-body MR scanner (Trio, A Tim System; Siemens Healthcare, Erlangen, Germany) using the body coil for radio frequency transmission and a 12-channel receive-only phased-array head coil for reception. Headphones were used to attenuate scanner noise. Foam pads were used to restrict head movement. In the second session, care was taken to place the subject in approximately the same position in the scanner and to prescribe the slices in approximately the same locations. To assess variability within each session, two baseline MR perfusion scans were acquired separately within a period of 20-30 min. This protocol was part of a larger study. Between the first and second perfusion scan, subjects underwent three different BOLD functional MRI scans for investigation of sensory motor and language function, which are not included in this report. No repositioning was performed for the second perfusion scan during each session while the subject remained in the scanner. All MR perfusion data were acquired in a resting state with closed eyes. Participants were instructed to hold still and keep awake without thinking about anything in particular.

Brain perfusion was measured with the product PASL sequence from Siemens as following: QUIPSS II (quantitative imaging of perfusion using a single subtraction, version 2), thin slice TI_1, periodic saturation (Q2TIPS) using a proximal inversion with a control for off-resonance effects (PICORE) labeling scheme (Luh et al., 1999). Using a 10-cm labeling region with 25 mm spacing from the distal edge of the labeled region to the image section, an adiabatic inversion pulse (FOCI) was employed for labeling followed by optimized inversion time delays TI_1 = 700 ms (time between the inversion pulse and the beginning of periodic saturation pulses), TI_1s = 1600 ms (time between the inversion pulse and the end of periodic saturation pulses), TI_2 = 1800 ms (time between the inversion pulse and acquisition of the proximal image), chosen so as to minimize intravascular signal intensity at 3T (Donahue et al., 2006; Wang et al., 2002). Interleaved label and control images were acquired using a gradient-echo single shot EPI readout, with acquisition parameters: TR/TE = 3000/13 ms, FOV = 224 mm, matrix = 64×64. The imaging region consisted of 16 contiguous ascending axial slices of 7 mm thickness. Each perfusion measurement consisted of 100 dynamics (50 control and label image pairs) plus one M_0 image (the equilibrium brain tissue magnetization used to normalize the difference perfusion map) with a scan time of approximately 5 minutes. The scanner's built-in 3D online prospective acquisition correction (PACE) was used to minimize head motion artifact during acquisition. In addition to perfusion imaging, each session included a high resolution T1-weighted magnetization prepared rapid gradient echo (MPRAGE) imaging with voxel size of 1×1×1.2 mm^3 for anatomical reference and a high resolution EPI whole brain scan with 2×2×2 mm^3 voxel size for subsequent image registration and normalization.

2.3. Image processing

Complex data were then reconstructed to magnitude EPI images (label/control) and then transferred to off-line workstation for analysis. All control and label images were realigned to the M_0 image with same spatial resolution from the same PASL acquisition. After that, the label images were pairwise subtracted from the time-matched control images to produce a perfusion weighted time series, and then quantitative rCBF map for each PASL scan, was generated using one compartment model (Wang et al., 2003b):

$$rCBF = \lambda \Delta M / (2 \alpha M_0 TI_1 \exp(-TI_2/T_{1a}))$$

Where ΔM is the mean difference in the signal intensity between label and control images, λ is the blood/tissue water partition coefficient, T_{1a} is the longitudinal relaxation time of

blood, α is the inversion efficiency and M_0 is the acquired voxelwise map. At 3T scanner, assumed values of λ = 0.9 ml/g, α = 95% and T_{1a} = 1500 ms primarily based on experience in healthy adults were applied (Wang et al., 2002). TI_2 increases incrementally per slice, with a slice repetition time of 36.5 ms

To compare inter- and intra-session rCBF maps across subjects, all rCBF maps were transformed into the Montréal Neurological Institute (MNI) standard space after a stepwise registration within the framework of SPM5 (Wellcome Department of Cognitive Neuroscience, London, UK). First, using the corresponding M_0 image as source image, two baseline rCBF maps were coregistered to the high resolution EPI reference image from the same session using mutual information function. Second, using the high resolution EPI image as source image, rCBF maps were coregistered to the T1-weighted MPRAGE image acquired during the same scan session. Next, rCBF maps from two different sessions were coregistered to the averaged T1-weighted MPRAGE image for each subject. It should be noted that during these steps no interpolation was applied to the data. Instead, only a set of parameters was estimated, which was applied later on. After that, the averaged MPRAGE imaging data were normalized onto the standard T1-weighted brain template image of SPM5 by using 12 nonlinear parametric transformations, resulting in spatially normalized isotropic MPRAGE images with 2 mm^3 spatial resolution. The parameters for normalization to MNI template were estimated based on the averaged T1-weighted MPRAGE image and transferred later to coregistered rCBF images. Then, rCBF images were normalized and resampled using nearest neighbor interpolation to a voxel size of with 2 mm^3, based on the application of parameters derived from the coregistration and normalization processes. To overcome small inconsistencies in registration, normalized rCBF data were spatially smoothed by using a 6 × 6 × 8 mm full width at half maximum (FWHM) kernel.

In addition, to differentiate between GM and white matter (WM) perfusion and to account for partial volumes of brain tissue and cerebrospinal fluid (CSF) in the perfusion-weighted imaging data, a segmentation algorithm combining anatomic information and signal intensity was applied to the T1-weighted MPRAGE images to obtain probabilistic GM, WM and CSF maps (Ashburner and Friston, 2005). Partial volume effects in rCBF maps were accounted for by filtering the coregistered perfusion-weighted imaging data with the probabilistic brain tissue masks generated using a threshold of 0.75 to yield rCBF maps including at least 75% GM and less than 25% other brain tissue, i.e. primarily WM and CSF (Jahng et al., 2005). rCBF maps were multiplied by the GM mask to obtain regional GM perfusion measurement.

Anatomical ROIs were delineated from 3D MPRAGE images using FreeSurfer (http://surfer.nmr.mgh.harvard.edu) (Fischl et al., 2002). Individual MPRAGE scans were processed using FreeSurfer through automated cortical parcellation to create accurate ROIs for each subject (Fischl et al., 2002). There are several stages to image processing through FreeSurfer. Briefly, the first stage involves intensity correction, normalization, Talairach transformation and skull stripping. Subcortical labeling occurs subsequent to these steps. Next, the white matter and pial surfaces are reconstructed and the final component involves cortical and subcortical labeling which result in total 36 cortical, 6 subcortical ROIs (Desikan et al., 2006; Fischl et al., 2004). All FreeSurfer ROI parcellation images were normalized into MNI space by applying same parameters estimated through normalization of MPRAGE as described above and then converted into a series of image masks with 2 mm^3 voxel resolution. Consistency of each ROI across subjects and scans was visually confirmed and size differences across all scans for each ROI were evaluated using the coefficient of variation (CV) defined as the ratio of the global mean divided by the standard deviation of all samples. Finally, these ROI masks were applied to perfusion data and the underlying rCBF distribution was extracted.

2.4. Statistical analysis

A key statistical issue to be addressed here is how consistent Q2TIPS PASL measurements are over repeated scans within- and between scan sessions. Popular terms for assessment of measurement properties include “reproducibility” and “reliability”, which are used with varying degrees of consistency in the literature of ASL technique (Floyd et al., 2003; Gevers et al., 2009; Hermes et al., 2007; Jahng et al., 2005; Parkes et al., 2004; Petersen et al., 2010; Xu et al., 2010; Yen et al., 2002). Mathematically, reliability relates the magnitude of the measurement error in observed measurements to the inherent variability in the underlying level of the quantity between subjects (Bartlett and Frost, 2008). Reproducibility is the variability of the average values obtained by several measurements while measuring the same item (Bartlett and Frost, 2008). Variability in measurements made on the same subject in a repeatability study can be ascribed only to errors due to the measurement process itself (Bartlett and Frost, 2008). Thus, in the present test-retest study, agreement between PASL measurements made on the same subject depends only on the within-subject SD, which measures the size of measurement errors (Bartlett and Frost, 2008).

The within-subject standard deviation (SD_W) was estimated by the formula $SD_W = (\Sigma(rCBF_{i1} - rCBF_{i2})^2/2n)^{0.5}$ (Bland and Altman, 1996), where n is the number of subjects and $rCBF_{i1} - rCBF_{i2}$ is the difference of rCBF between two scans for subject i. The repeatability index (RI) was defined as the 95% confidence interval (CI) for repeated measurements given by: $RI = 1.96 \times SD_W$, where SD_W is the within subject standard deviation of the rCBF difference between repeated measurements (Bland and Altman, 1996; Gevers et al., 2009). The RI reflects the largest difference between measurements that is likely due to measurement error. In addition, the within-subject coefficient of variation (CV_W) that quantifies measurement error relative to the size of rCBF was also calculated as: $CV_W = SDW/\mu \times 100\%$, where μ is the mean rCBF per ROI, to simplify comparisons with data in other reports of reproducibility in ASL perfusion imaging (Jahng et al., 2005; Petersen et al., 2010). In comparison, between-subject standard deviation (SD_B) of the mean rCBF per ROI was also estimated. Furthermore, intra- and inter-session reliability was also assessed using intra-class correlation coefficients (ICC) estimated with variance components models. As described by Jahng et al. (Jahng et al., 2005), the reliability was computed as an intraclass correlation coefficient (ICC), according to the equation following the original concept of Shrout and Fleiss (Shrout and Fleiss, 1979):

$$ICC = n(\sigma_n^2 - \sigma_\varepsilon^2)/\sigma_{tot}^2 .$$

Here,

$$\sigma_{tot}^2 = n(\sigma_n^2 - \sigma_\varepsilon^2) + k(\sigma_k^2 - \sigma_\varepsilon^2) + nk\sigma_\varepsilon^2 ,$$

where n and k are the numbers of subjects and scans, respectively; σ_n^2 is the variance between subjects, σ_k^2 is the within-subject scan variance due to test and retest, σ_ε^2 is the variance due to random noise. An ICC of near unity indicates high reliability (an ICC of 1.0 indicates perfect reliability), whereas a value of 0.5 or lower indicates a significant contribution of random error that has diminished usefulness in distinguishing among subjects (Jahng et al., 2005). To assess intrasession reliability and reproducibility, we compared rCBF values obtained from the first and the second scans within each session, and to assess intersession reproducibility, we compared mean rCBF values of the first, second sessions. Above statistical analyses were conducted for whole brain GM and each ROI,

respectively. All statistical analyses were performed using SPSS for Windows (Version 16.0, SPSS Inc., Chicago, IL).

3. Results

3.1.1 Global and lobar cortical regions

Global mean cortical grey matter rCBF was 58.5 ± 9.9 ml/100g/min (Mean ± SD_B, where SD_B = between-subject standard deviation) which is found to be within the range of previous studies using PASL (Campbell and Beaulieu, 2006; Figueiredo et al., 2005; Yen et al., 2002) and PET MRI comparison study (Donahue et al., 2006; Xu et al., 2010). Female participants showed higher global cortical GM rCBF values than males (63.3 ± 11.5 vs. 53.6 ± 5.6 ml/100g/min, $p < 0.01$), consistent with longstanding observations (Gur et al., 1982). The reliability, expressed as ICC; reproducibility, indicated as SD_W, RI and CV_W of perfusion measurements obtained with PASL method in global cortical GM, and each lobar cortex are summarized in Table 1. For global cortical GM rCBF measurement, intersession and intrasession ICC were 0.90 and 0.95, intersession RI was 6.5 ml/100g/min with CV_W of 5.7%, intrasession RI and CV_W were 3.3 ml/100g/min and 2.9%. Intersession and intrasession ICCs for lobar regions were within the range of 0.85 ~ 0.91 and 0.87 ~ 0.95. RI varied from 6.7 to 11.5 ml/100g/min for intersession and 3.9 to 9.1 ml/100g/min for intrasession comparison, while intersession and intrasession CV_W were within 5.9% to 7.0% and 3.2% to 5.6%. For global and any lobar cortical region, SD_B was greater than SD_W. As we expected, intrasession comparison showed slightly better reproducibility than intersession comparison. Relatively lower inter- and intrasession reproducibility found in occipital lobe. Overall, these results at the lobar level indicated high reliability and reproducibility between inter- and intrasession PASL scans for MR perfusion measurement. Results are consistent with previous results reported using CASL with comparable study design (Gevers et al., 2009). In any given ROI, within-subject standard deviation is less than between-subject standard deviation (Fig. 1).

3.1.2. Subdivisions of neocortex

The results for neocortical ROIs are summarized in Table 2. Clearly, rCBF values varied across regions. The reliability and reproducibility estimations were unevenly distributed across subdivisions in neocortex. Compared to the estimation at lobar level, both inter- and intrasession ICC in subdivisional cortical ROIs showed greater variability ranged from 0.68 to 0.95, while majority of subregions showed inter- and intrasession ICC greater than 0.80. Several ROIs in parietal or temporal lobe demonstrated inter- and intrasession ICC above 0.90 with relatively small RI and CV_W. There are only a few regions showing ICC less than 0.75. Lowest intersession ICC (0.68) with relatively high CV_W (10.2%) was found in superior frontal gyrus, while intrasession ICC, CV_W of the same region was at the intermediate level (0.82 and 6.4%). Interestingly, inferior frontal ROIs, particularly pars opercularis and pars triangularis, showed intrasession ICC lower than intersession one, with intrasession SD_W and CV_W higher than intersession one. The caudal middle frontal ROI showed low inter- and intra-session (0.72 and 0.73) with moderately high CV_W (7.9% and 7.2%), while posterior cingulate cortex demonstrated the same level of inter- and intra-session (0.73 and 0.72) with relatively larger RI (12.7 ml/100g/min and 12.2 ml/100g/min) and higher CV_W (9.4% and 8.9%). Caudal anterior cingulate ROI also showed fairly large intersession within-subject variability with ICC of 0.71, RI of 13.3 ml/100g/min and CV_W of 12.1%. For any subregion ROI, SD_B was greater than SD_W. In additional correlation analysis, we only found modest negative correlation between ROI grey matter volume and inter-session SD_w for frontal ROIs ($r = -0.56$, $p = 0.049$).

3.1.3. Subcortical regions

In subcortical areas (Table 3), hippocampus showed relatively stable intersession and intrasession rCBF variability (ICC: 0.88 vs. 0.85; CV_W: 6% vs. 5.1%). Amygdala presented rather less stable intersession and intrasession rCBF with moderately low ICC and CV_W. The most variable rCBF was detected in thalamus ROI with lowest intersession and intrasession ICC (0.72 vs. 0.66), highest intrasession RI (18.8 ml/100g/min vs. 17.2 ml/100g/min) and CV_W (10.8% vs. 11.6%). Striatum regions including caudate and putamen also demonstrated more intrasession variability compared to intersession estimation. No significant correlation between grey matter volume and SD_w was found for subcortical ROIs.

4. Discussion

Multislice PICORE Q2TIPS is a widely used PASL technique that has been reported to yield accurate and efficient quantification of rCBF (Campbell and Beaulieu, 2006). Using a test-retest study design, we have examined inter- and intra-session variation in rCBF measurement using PICORE Q2TIPS in GM of cortical and subcortical ROIs derived from an automated parcellation approach using individual high resolution anatomical MR images. Our between session reproducibility findings are commensurate with previous reports with similar designs (Floyd et al., 2003; Gevers et al., 2009; Hermes et al., 2007; Petersen et al., 2010; Yen et al., 2002). Similarly within session reliability is also consistent with recent reports examining intra-session variation in rCBF changes at global and lobar level (Gevers et al., 2009). To our best knowledge, this report is the first one that combines within and between session rCBF variability measurements with individualized anatomically defined ROIs, including subcortical regions.

Variation between subjects is most important when a comparison of rCBF between populations is planned, such as in patient vs. control studies. However, when considering repeated measurements on the same subject, such as in longitudinal studies (Petersen et al., 2010) within-subject variation is critically important. The volume of brain structures on anatomical MRI typically has minimal variability during short time intervals, at least under normal conditions, whereas perfusion can fluctuate considerably, depending on brain activity and other factors. Therefore, physiologic variability in rCBF may cause reduced and reproducibility and reliability of measurement (Jahng et al., 2005). In the present study, we have estimated within-subject deviation of rCBF, along with RI and CV_W to express reproducibility. While SD_W varied within relatively small range, the reliability index ICC was greater than 0.80 in most regions. In any given ROI, within-subject standard deviation is less than between-subject standard deviation. Since the ICC can be interpreted as the proportion of variability explained by subject differences as opposed to measurement error and random noise (Bartlett and Frost, 2008), our results suggest that all other variations (that can't be explained by within-subject effect) is the greater contributor to fluctuations in perfusion signal rather than within-subject effects. This finding supports the notion that GM perfusion variation between individuals is large. The exact cause of this variation remains elusive. It could be linked to biologic origin, such as individual differences in blood T1 or variation in neuronal density or number (Parkes et al., 2004), or it also could be due to individual differences in underlying physiological fluctuation (Petersen et al., 2010). Asllani, et al. have suggested that the variability of rCBF values across regions can be due to an inverse relationship between ROI volume and intrasubject variance (Asllani et al., 2008b). Unlike their study using a publicly available ROI template, the current work applied individualized ROIs. Our results showed no significant correlation between ROI volume and within-subject standard deviation of rCBF per ROI in most regions.

Since intrasession scans were repeated without repositioning, the potential error from acquisition plane was averted. As expected, intrasessional reliability and reproducibility are generally better than those between sessions. However, they are closely comparable in most regions. Interestingly, compared with other ROIs within same lobe, slightly lower intrasession reliability and reproducibility with relatively higher within-subject variability were evident in posterior cingulate cortex, inferior frontal gyrus and caudal middle frontal gyrus. Furthermore, subcortical regions showed more limited intrasession reliability and reproducibility in thalamus, putamen and right caudate. We speculate that this spatial nonuniformity of reliability and reproducibility in resting rCBF measurement are mainly owing to following factors. First, it has been observed that ASL perfusion MRI data obtained at rest also demonstrate increased activity in the default mode network (DMN) consisted of both medial (including posterior cingulate and medial frontal cortex) and lateral brain regions (including inferior frontal cortex) (Detre et al., 2009). The DMN was initially observed using PET scanning, but has since been observed in BOLD functional MRI both by contrasting baseline to task and by examining functional connectivity patterns (Fox et al., 2006). It should be mentioned, there were three different fMRI studies between two PASL scans within each session of the current study. While differences in arousal could account for some of the individual perfusion differences (Parkes et al., 2004), there is also evidence showing that preceding cognitive load can alter subsequent activity in DMN (Pyka et al., 2009). Second, one recent study using independent component analysis has illustrated a partial decoupling across subjects in levels of perfusion in posterior parts of the brain correspond to the territory of the posterior cerebral artery (Viviani et al., 2009). The differential pattern of perfusion of these regions may be explained by the fact that the supply of the posterior cerebral artery differs markedly from the supply of the other arterial vessels of the brain. (Viviani et al., 2009). Third, higher magnetic susceptibility due to intracranial cavities, which cause both signal intensity variations and geometric distortions at perfusion-weighted imaging, is the most likely reason for the lower reliability in amygdala and lower part of inferior frontal cortex (Jahng et al., 2005). In addition, possible subject motion and acquisition errors can also be attributable to the variability in rCBF values (Petersen et al., 2010). Poorer reliability and reproducibility of PASL measurement in some subcortical ROIs might be as results of coregistration errors and / or partial volume effects. Also due to partial brain coverage of the Q2TIPS PASL, these ROIs at the lowest slices may not be consistently acquired.

Given the limited spatial resolution in PASL imaging, grey matter rCBF can be underestimated at lower resolution owing to partial volume contributions from WM and CSF (Donahue et al., 2006; Shin et al., 2007). To minimize the partial volume averaging, we have adopted methods from other reproducibility studies of MR perfusion (Jahng et al., 2005; Shin et al., 2007), where only voxels with larger than a threshold of 0.75 in GM type were considered in tissue probability mask. However, there were no voxels in bilateral globus pallidum ROI obtained from Freesurfer that survived the 0.75 GM threshold in six subjects of this study. Therefore, the globus pallidum was excluded from further analysis. Recently, a few complex algorithms have been developed for correction of partial volume effect in ASL imaging (Alsop et al., 2008; Asllani et al., 2008a), which could be relevant especially in studies of elderly subjects where atrophy can be a factor in the rCBF difference observed (Alsop et al., 2008). Future work is warranted to investigate how reliability of the PASL scan can be improved by applying different partial volume correction.

Like other dynamic MRI scans, the ASL signal can be modulated by physiological noise (Restom et al., 2006). Wu, et al. have inspected the pulsed ASL data at resting state with prospective gating and showed that cardiac pulsation could confound ASL signals via the variant amount of tags delivered into imaging slices (Wu et al., 2007b). While the interleaved acquisition of label or control images tends to whiten physiological noise and as

a result mean rCBF may be largely unaffected for measurements of one PASL scan over a few minutes (Wu et al., 2009). It remains an open question to what extent the physiological noise correction is useful for baseline rCBF measurement, which merits further investigation.

This study was carried out at 3T with the advantage of longer T1-weighted relaxation times and higher signal-to-noise ratio compared to 1.5T. Other PASL technique related factors might be considered which can also influence the quality of MRI rCBF results. These issues include the post-labeling delay, magnetization transfer contributions, arrival time and labeling efficiency (Donahue et al., 2006; Parkes et al., 2004). However, the exact contributions of acquisition and physiology-related variability remain unclear and more knowledge of underlying mechanisms will be essential (Campbell and Beaulieu, 2006; Donahue et al., 2006; Gevers et al., 2009). The problem of isolating measurement error from physiologic fluctuations was not addressed in the present study design. We have used consistently the T1a value of 1500ms derived from the study of Wang and his colleagues (Wang et al., 2002), though more recent experimental data indicated an 11% higher T1a value at 3T (Lu et al., 2004). This would not affect the conclusions of the current paper regarding reproducibility, but could potentially bias the absolute rCBF values. Absolute rCBF values are however highly dependent on the method and input data used and thus scale differently (Cavusoglu et al., 2009).

5. Conclusions

In summary, our findings indicated good reproducibility of MR perfusion measurements using the PICORE Q2TIPS PASL technique. A number of factors can influence rCBF values, considerable region dependent variability in grey matter rCBF has also been demonstrated. Regional differences in reproducibility should be taken into account in future research of specific applications using PASL perfusion measurement as a biomarker. Our results provide a framework for such assessments.

Acknowledgments

Data analysis was supported in part by the following grants from the National Institutes of Health: NIA R01 AG19771 and NCI R01 CA101318 to AJS, P30 AG10133-18S1 to B. Ghetti/AJS, NIBIB R03 EB008674 to LS and Indiana Economic Development Corporation (#87884) to AJS.

References

Alsop DC, Casement M, de Bazelaire C, Fong T, Press DZ. Hippocampal hyperperfusion in Alzheimer's disease. Neuroimage. 2008; 42:1267–1274. [PubMed: 18602481]

Ashburner J, Friston KJ. Unified segmentation. Neuroimage. 2005; 26:839–851. [PubMed: 15955494]

Asllani I, Borogovac A, Brown TR. Regression algorithm correcting for partial volume effects in arterial spin labeling MRI. Magn Reson Med. 2008a; 60:1362–1371. [PubMed: 18828149]

Asllani I, Borogovac A, Wright C, Sacco R, Brown TR, Zarahn E. An investigation of statistical power for continuous arterial spin labeling imaging at 1.5 T. Neuroimage. 2008b; 39:1246–1256. [PubMed: 18036834]

Bartlett JW, Frost C. Reliability, repeatability and reproducibility: analysis of measurement errors in continuous variables. Ultrasound Obstet Gynecol. 2008; 31:466–475. [PubMed: 18306169]

Bland JM, Altman DG. Measurement error. BMJ. 1996; 313:744. [PubMed: 8819450]

Brown GG, Clark C, Liu TT. Measurement of cerebral perfusion with arterial spin labeling: Part 2. Applications. Journal of the International Neuropsychological Society. 2007; 13:526–538. [PubMed: 17445302]

Campbell AM, Beaulieu C. Comparison of multislice and single-slice acquisitions for pulsed arterial spin labeling measurements of cerebral perfusion. Magn Reson Imaging. 2006; 24:869–876. [PubMed: 16916704]

Cavusoglu M, Pfeuffer J, Ugurbil K, Uludag K. Comparison of pulsed arterial spin labeling encoding schemes and absolute perfusion quantification. Magn Reson Imaging. 2009; 27:1039–1045. [PubMed: 19540694]

Dai W, Garcia D, Bazelaire Cd, Alsop DC. Continuous flow-driven inversion for arterial spin labeling using pulsed radio frequency and gradient fields. Magn Reson Med. 2008; 60:1488–1497. [PubMed: 19025913]

Desikan RS, Segonne F, Fischl B, Quinn BT, Dickerson BC, Blacker D, Buckner RL, Dale AM, Maguire RP, Hyman BT, Albert MS, Killiany RJ. An automated labeling system for subdividing the human cerebral cortex on MRI scans into gyral based regions of interest. Neuroimage. 2006; 31:968–980. [PubMed: 16530430]

Detre JA, Leigh JS, Williams DS, Koretsky AP. Perfusion imaging. Magn Reson Med. 1992; 23:37–45. [PubMed: 1734182]

Detre JA, Wang J, Wang Z, Rao H. Arterial spin-labeled perfusion MRI in basic and clinical neuroscience. Current Opinion in Neurology. 2009; 22:348–355. [PubMed: 19491678]

Donahue MJ, Lu H, Jones CK, Pekar JJ, van Zijl PC. An account of the discrepancy between MRI and PET cerebral blood flow measures. A high-field MRI investigation. NMR in Biomedicine. 2006; 19:1043–1054. [PubMed: 16948114]

Du AT, Jahng GH, Hayasaka S, Kramer JH, Rosen HJ, Gorno-Tempini ML, Rankin KP, Miller BL, Weiner MW, Schuff N. Hypoperfusion in frontotemporal dementia and Alzheimer disease by arterial spin labeling MRI. Neurology. 2006; 67:1215–1220. [PubMed: 17030755]

Figueiredo PM, Clare S, Jezzard P. Quantitative perfusion measurements using pulsed arterial spin labeling: effects of large region-of-interest analysis. Journal of Magnetic Resonance Imaging. 2005; 21:676–682. [PubMed: 15906323]

Fischl B, Salat DH, Busa E, Albert M, Dieterich M, Haselgrove C, van der Kouwe A, Killiany R, Kennedy D, Klaveness S, Montillo A, Makris N, Rosen B, Dale AM. Whole brain segmentation: automated labeling of neuroanatomical structures in the human brain. Neuron. 2002; 33:341–355. [PubMed: 11832223]

Fischl B, van der Kouwe A, Destrieux C, Halgren E, Segonne F, Salat DH, Busa E, Seidman LJ, Goldstein J, Kennedy D, Caviness V, Makris N, Rosen B, Dale AM. Automatically parcellating the human cerebral cortex. Cereb Cortex. 2004; 14:11–22. [PubMed: 14654453]

Floyd TF, Ratcliffe SJ, Wang J, Resch B, Detre JA. Precision of the CASL-perfusion MRI technique for the measurement of cerebral blood flow in whole brain and vascular territories. Journal of Magnetic Resonance Imaging. 2003; 18:649–655. [PubMed: 14635149]

Fox MD, Snyder AZ, Zacks JM, Raichle ME. Coherent spontaneous activity accounts for trial-to-trial variability in human evoked brain responses. Nat Neurosci. 2006; 9:23–25. [PubMed: 16341210]

Gevers S, Majoie CB, van den Tweel XW, Lavini C, Nederveen AJ. Acquisition time and reproducibility of continuous arterial spin-labeling perfusion imaging at 3T. American Journal of Neuroradiology. 2009; 30:968–971. [PubMed: 19193760]

Gur RC, Gur RE, Obrist WD, Hungerbuhler JP, Younkin D, Rosen AD, Skolnick BE, Reivich M. Sex and handedness differences in cerebral blood flow during rest and cognitive activity. Science. 1982; 217:659–661. [PubMed: 7089587]

Hermes M, Hagemann D, Britz P, Lieser S, Rock J, Naumann E, Walter C. Reproducibility of continuous arterial spin labeling perfusion MRI after 7 weeks. MAGMA. 2007; 20:103–115. [PubMed: 17429703]

Jahng GH, Song E, Zhu XP, Matson GB, Weiner MW, Schuff N. Human brain: reliability and reproducibility of pulsed arterial spin-labeling perfusion MR imaging. Radiology. 2005; 234:909–916. [PubMed: 15734942]

Liu TT, Brown GG. Measurement of cerebral perfusion with arterial spin labeling: Part 1. Methods. Journal of the International Neuropsychological Society. 2007; 13:517–525. [PubMed: 17445301]

Lu H, Clingman C, Golay X, van Zijl PC. Determining the longitudinal relaxation time (T1) of blood at 3.0 Tesla. Magn Reson Med. 2004; 52:679–682. [PubMed: 15334591]

Luh WM, Wong EC, Bandettini PA, Hyde JS. QUIPSS II with thin-slice TI1 periodic saturation: a method for improving accuracy of quantitative perfusion imaging using pulsed arterial spin labeling. Magn Reson Med. 1999; 41:1246–1254. [PubMed: 10371458]

Parkes LM, Rashid W, Chard DT, Tofts PS. Normal cerebral perfusion measurements using arterial spin labeling: reproducibility, stability, and age and gender effects. Magn Reson Med. 2004; 51:736–743. [PubMed: 15065246]

Petersen ET, Mouridsen K, Golay X. The QUASAR reproducibility study, Part II: Results from a multi-center Arterial Spin Labeling test-retest study. Neuroimage. 2010; 49:104–113. [PubMed: 19660557]

Petersen ET, Zimine I, Ho YC, Golay X. Non-invasive measurement of perfusion: a critical review of arterial spin labelling techniques. British Journal of Radiology. 2006; 79:688–701. [PubMed: 16861326]

Pyka M, Beckmann CF, Schoning S, Hauke S, Heider D, Kugel H, Arolt V, Konrad C. Impact of working memory load on FMRI resting state pattern in subsequent resting phases. PLoS One. 2009; 4:e7198. [PubMed: 19779619]

Restom K, Behzadi Y, Liu TT. Physiological noise reduction for arterial spin labeling functional MRI. Neuroimage. 2006; 31:1104–1115. [PubMed: 16533609]

Shin W, Horowitz S, Ragin A, Chen Y, Walker M, Carroll TJ. Quantitative cerebral perfusion using dynamic susceptibility contrast MRI: evaluation of reproducibility and age- and gender-dependence with fully automatic image postprocessing algorithm. Magn Reson Med. 2007; 58:1232–1241. [PubMed: 17969025]

Shrout PE, Fleiss JL. Intraclass correlations: uses in assessing rater reliability. Psychol Bull. 1979; 86:420–428. [PubMed: 18839484]

Tjandra T, Brooks JC, Figueiredo P, Wise R, Matthews PM, Tracey I. Quantitative assessment of the reproducibility of functional activation measured with BOLD and MR perfusion imaging: implications for clinical trial design. Neuroimage. 2005; 27:393–401. [PubMed: 15921936]

Viviani R, Sim EJ, Lo H, Richter S, Haffer S, Osterfeld N, Thone J, Beschoner P. Components of variance in brain perfusion and the design of studies of individual differences: the baseline study. Neuroimage. 2009; 46:12–22. [PubMed: 19457381]

Wang J, Aguirre GK, Kimberg DY, Roc AC, Li L, Detre JA. Arterial spin labeling perfusion fMRI with very low task frequency. Magn Reson Med. 2003a; 49:796–802. [PubMed: 12704760]

Wang J, Alsop DC, Li L, Listerud J, Gonzalez-At JB, Schnall MD, Detre JA. Comparison of quantitative perfusion imaging using arterial spin labeling at 1.5 and 4.0 Tesla. Magn Reson Med. 2002; 48:242–254. [PubMed: 12210932]

Wang J, Licht DJ, Jahng GH, Liu CS, Rubin JT, Haselgrove J, Zimmerman RA, Detre JA. Pediatric perfusion imaging using pulsed arterial spin labeling. Journal of Magnetic Resonance Imaging. 2003b; 18:404–413. [PubMed: 14508776]

Williams DS, Detre JA, Leigh JS, Koretsky AP. Magnetic resonance imaging of perfusion using spin inversion of arterial water. Proceedings of the National Academy of Sciences of the United States of America. 1992; 89:212–216. [PubMed: 1729691]

Wintermark M, Sesay M, Barbier E, Borbely K, Dillon WP, Eastwood JD, Glenn TC, Grandin CB, Pedraza S, Soustiel JF, Nariai T, Zaharchuk G, Caille JM, Dousset V, Yonas H. Comparative Overview of Brain Perfusion Imaging Techniques. Stroke. 2005; 36:e83–99. [PubMed: 16100027]

Wong EC, Buxton RB, Frank LR. Quantitative imaging of perfusion using a single subtraction (QUIPSS and QUIPSS II). Magn Reson Med. 1998; 39:702–708. [PubMed: 9581600]

Wong EC, Buxton RB, Frank LR. Quantitative perfusion imaging using arterial spin labeling. Neuroimaging Clinics of North America. 1999; 9:333–342. [PubMed: 10318718]

Wu WC, Edlow BL, Elliot MA, Wang J, Detre JA. Physiological modulations in arterial spin labeling perfusion magnetic resonance imaging. IEEE Trans Med Imaging. 2009; 28:703–709. [PubMed: 19150788]

Wu WC, Fernandez-Seara M, Detre JA, Wehrli FW, Wang J. A theoretical and experimental investigation of the tagging efficiency of pseudocontinuous arterial spin labeling. Magn Reson Med. 2007a; 58:1020–1027. [PubMed: 17969096]

Wu WC, Mazaheri Y, Wong EC. The effects of flow dispersion and cardiac pulsation in arterial spin labeling. IEEE Trans Med Imaging. 2007b; 26:84–92. [PubMed: 17243587]

Xu GF, Rowley HA, Wu GH, Alsop DC, Shankaranarayanan A, Dowling M, Christian BT, Oakes TR, Johnson SC. Reliability and precision of pseudo-continuous arterial spin labeling perfusion MRI on 3.0 T and comparison with O-15-water PET in elderly subjects at risk for Alzheimer's disease. NMR in Biomedicine. 2010; 23:286–293. [PubMed: 19953503]

Yen YF, Field AS, Martin EM, Ari N, Burdette JH, Moody DM, Takahashi AM. Test-retest reproducibility of quantitative CBF measurements using FAIR perfusion MRI and acetazolamide challenge. Magn Reson Med. 2002; 47:921–928. [PubMed: 11979571]

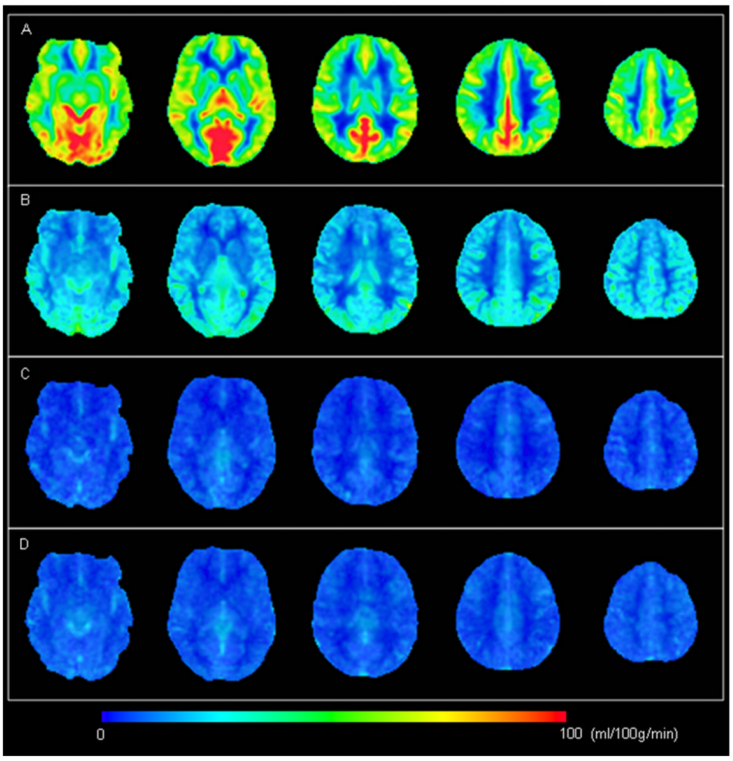

Figure 1.
Brain images illustrate estimates of average rCBF (a); between-subject standard deviation of rCBF (b); between-session within-subject standard deviation of rCBF (c); and within-session within-subject standard deviation of rCBF (d). Data were normalized into MNI space and spatially smoothed.

Table 1

Average volume (Mean ± SD_B, cm^3), average rCBF (Mean ± SD_B, ml/100g/min), intersession and intrasession reliability and reproducibility of rCBF measurement in global cortical and lobar cortex grey matter regions.

Regions	Volume (grey matter)	rCBF	Intersession				Intrasession			
			ICC	SD_W	RI	CV_W	ICC	SD_W	RI	CV_W
Global Cortical Cortex	615.8 ± 44.5	58.5 ± 9.9	0.90	3.3	6.5	5.7%	0.95	1.7	3.3	2.9%
Frontal Lobe	89.2 ± 20.5	52.4 ± 8.9	0.85	3.4	6.7	6.5%	0.91	2.0	3.9	3.8%
Parietal Lobe	55.9 ± 13.2	62.6 ± 12.6	0.91	4.2	8.3	6.8%	0.95	2.0	3.9	3.2%
Temporal Lobe	68.1 ± 10.6	59.7 ± 10	0.90	3.5	6.9	5.9%	0.90	2.4	4.8	4.0%
Occipital Lobe	29.2 ± 6.1	83.6 ± 16.8	0.87	5.9	11.5	7.0%	0.87	4.6	9.1	5.6%

Note: SD_B, between-subject standard deviation; ICC, intraclass correlation coefficient; SD_W, within-subject standard deviation; RI, repeatability index; CV_W, within-subject coefficient of variation;

Table 2

Average volume (Mean ± SD_B, cm^3), average rCBF (Mean ± SD_B, ml/100g/min), intersession and intrasession reliability and reproducibility of rCBF measurement in cortical grey matter regions.

Regions	Volume (grey matter)	rCBF	Intersession				Intrasession			
			ICC	SD_W	RI	CV_W	ICC	SD_W	RI	CV_W
Frontal Lobe										
Superior frontal gyrus	23.8 ± 5.7	47.0 ± 8.6	0.68	4.8	9.4	10.2%	0.82	3.0	5.9	6.4%
Middle frontal gyrus	22.9 ± 6	57.1 ± 9.8	0.82	3.9	7.7	6.9%	0.84	3.0	5.9	5.3%
Rostral middle frontal	16.8 ± 4.3	56.9 ± 10.1	0.84	3.9	7.6	6.8%	0.84	3.0	5.8	5.2%
Caudal middle frontal	6.2 ± 1.8	57.6 ± 9.8	0.72	4.5	8.9	7.9%	0.73	4.2	8.2	7.2%
Inferior frontal gyrus	11.7 ± 2.5	61.7 ± 10.0	0.83	4.0	7.9	6.5%	0.76	4.0	7.9	6.5%
Pars opercularis	5.8 ± 1.1	63.5 ± 10.8	0.77	4.9	9.7	7.8%	0.68	5.2	10.1	8.1%
Pars triangularis	3.8 ± 1	60.2 ± 9.7	0.78	4.3	8.4	7.2%	0.69	4.6	9.1	7.6%
Pars orbitalis	2.1 ± 0.5	59.5 ± 9.6	0.84	2.8	5.6	4.8%	0.76	3.7	7.2	6.2%
Orbitofrontal cortex	14.3 ± 2.5	47.6 ± 8.4	0.91	2.1	4.0	4.3%	0.85	2.5	5.0	5.1%
Lateral division	9.7 ± 1.6	51.0 ± 8.7	0.90	2.0	3.9	3.9%	0.83	2.8	5.5	5.4%
Medial division	4.6 ± 0.9	40.3 ± 9.0	0.88	2.7	5.3	6.7%	0.85	2.7	5.2	6.1%
Precentral gyrus	12.8 ± 3.5	52.2 ± 10.4	0.87	3.4	6.6	6.4%	0.88	2.7	5.2	5.1%
Paracentral lobule	3.7 ± 0.9	47.1 ± 13.7	0.82	4.9	9.5	10.3%	0.82	4.5	8.8	9.6%
Parietal Lobe										
Postcentral gyrus	7.8 ± 2.4	52.5 ± 12.6	0.88	4.1	8.1	7.8%	0.93	2.5	5.0	4.7%
Supramarginal gyrus	12.0 ± 2.6	58.7 ± 12.1	0.90	4.5	8.9	7.7%	0.94	2.2	4.3	3.7%
Superior parietal cortex	9.1 ± 3.3	53.6 ± 13.0	0.90	4.3	8.4	8.0%	0.91	2.9	5.7	5.4%
Inferior parietal cortex	14.9 ± 3.1	61.5 ± 14.9	0.94	4.2	8.3	6.9%	0.95	2.4	4.6	3.7%
Precuneus cortex	12.1 ± 2.0	80.5 ± 14.7	0.81	6.4	12.6	8.0%	0.84	4.4	8.6	5.3%
Temporal Lobe										
Superior temporal gyrus	18.4 ± 3.4	59.4 ± 11.9	0.88	4.4	8.7	7.5%	0.86	3.4	6.6	5.7%
Middle temporal gyrus	15.2 ± 2.4	57.2 ± 11.0	0.91	3.8	7.4	6.6%	0.94	2.1	4.1	3.7%
Inferior temporal gyrus	15.3 ± 2.7	45.6 ± 9.8	0.89	3.0	6.0	6.7%	0.85	3.0	5.8	6.5%
Transverse temporal cortex	1.7 ± 0.3	79.7 ± 16.5	0.85	6.9	13.5	8.6%	0.84	5.2	10.2	6.0%
Parahippocampal gyrus	3.0 ± 0.2	70.9 ± 11.4	0.77	5.5	10.8	7.8%	0.82	3.8	7.4	5.3%

Regions	Volume (grey matter)	rCBF	Intersession				Intrasession			
			ICC	SD_W	RI	CV_W	ICC	SD_W	RI	CV_W
Entorhinal cortex	2.4 ± 0.2	40.9 ± 13.8	0.92	3.9	7.6	9.5%	0.92	2.9	5.6	7.0%
Fusiform gyrus	14.6 ± 2.0	72.6 ± 13.7	0.90	4.1	8.1	5.7%	0.87	3.8	7.4	5.2%
Occipital Lobe										
Lingual gyrus	11.0 ± 1.6	93.9 ± 18.4	0.86	6.4	12.5	6.8%	0.87	5.0	9.8	5.3%
Pericalcarine cortex	2.9 ± 0.9	95.0 ± 19.7	0.87	7.2	14.1	7.6%	0.90	5.0	9.9	5.2%
Cuneus cortex	4.5 ± 1.1	91.1 ± 18.2	0.88	6.0	11.7	6.6%	0.87	5.2	10.2	5.6%
Lateral occipital cortex	10.8 ± 2.7	66.2 ± 15.9	0.85	5.6	11.1	8.5%	0.83	5.2	10.2	7.8%
Cingulate Cortex	16.3 ± 1.8	69.5 ± 12.3	0.78	5.7	11.2	8.2%	0.87	3.5	6.8	4.9%
Rostral anterior division	3.6 ± 0.5	60.3 ± 10.5	0.77	5.5	10.7	9.1%	0.80	4.0	7.9	6.6%
Caudal anterior division	3.2 ± 0.5	56.2 ± 12.3	0.71	6.8	13.3	12.1%	0.87	3.5	6.9	6.3%
Posterior division	6.1 ± 0.6	69.1 ± 14.0	0.73	6.5	12.7	9.4%	0.72	6.2	12.2	8.9%

Note: SD_B, between-subject standard deviation; ICC, intraclass correlation coefficient; SD_W, within-subject standard deviation; RI, repeatability index; CV_W, within-subject coefficient of variation;

Table 3

Average size (Mean ± SD_B, cm^3), average rCBF (Mean ± SD_B, ml/100g/min), intersession and intrasession reliability and reproducibility of rCBF measurement in subcortical grey matter regions.

Regions	Volume (grey matter)	rCBF	Intersession				Intrasession			
			ICC	SD_W	RI	CV_W	ICC	SD_W	RI	CV_W
Caudate	6.3 ± 1.2	42.4 ± 6.8	0.81	2.7	5.4	6.5%	0.79	2.3	4.6	5.3%
Putamen	6.8 ± 1.1	50.2 ± 8.6	0.83	2.6	5.2	5.3%	0.74	3.5	6.8	6.9%
Thalamus	4.8 ± 0.6	81.5 ± 20.0	0.72	8.8	17.2	10.8%	0.66	9.6	18.8	11.6%
Amygdala	4.1 ± 0.2	48.5 ± 9.6	0.77	4.6	9.1	9.6%	0.78	3.9	7.6	7.9%
Hippocampus	7.5 ± 0.4	70.2 ± 12.7	0.88	4.2	8.2	6.0%	0.85	3.6	7.1	5.1%

Note: SD_B, between-subject standard deviation; ICC, intraclass correlation coefficient; SD_W, within-subject standard deviation; RI, repeatability index; CV_W, within-subject coefficient of variation;